

A new xandarellid euarthropod from the Cambrian Chengjiang biota,
Yunnan Province, China

XIANGUANG HOU^{*}, MARK WILLIAMS[†], ROBERT SANSOM[§], DEREK J.
SIVETER^{‡,β}, DAVID J. SIVETER[†], SARAH GABBOTT[†], THOMAS H.P.
HARVEY[†], PEIYUN CONG^{*II}, YU LIU^{*¶}

^{*}Yunnan Key Laboratory for Palaeobiology, Yunnan University, Kunming 650091, China

[†]School of Geography, Geology and the Environment, University of Leicester, Leicester LE1
7RH, UK

[§]School of Earth and Environmental Sciences, University of Manchester, Oxford Road, M13
9PT, UK

[‡]Earth Collections, Oxford University Museum of Natural History, Parks Road, Oxford, OX1
3PW, UK

^βDepartment of Earth Sciences, University of Oxford, South Parks Road, Oxford OX1 3PR,
UK

^{II}The Natural History Museum, Cromwell Road, South Kensington, London, SW7 5BD, UK

¶ Author for correspondence: yu.liu@ynu.edu.cn

Abstract

The euarthropod *Luohuilinella deletres* sp. nov. is described from rare material from the Chengjiang biota, Cambrian Series 2, Stage 3, of Yunnan Province, China. Phylogenetic analysis recovers a xandarellid affinity for *L. deletres*, representing only the fifth described species of this clade. *L. deletres* possesses a head shield that is about one-fifth of the total body length and a trunk with 30 tergites, the reduced anterior-most tergite and terminal three tergites lacking pleural elongations. Anteriorly situated notches in the head shield are associated with stalked eyes, in contrast to the more posterior, enclosed eye slits present in *Xandarella*. Posterior to the antennae there are at least eleven pairs of biramous appendages preserved, including three pairs in the head. The morphology of the midline gut of *L. deletres*, in

which lateral, unbranched diverticula are wider towards the front of the body, is a character also found in various trilobites. The dorsoventrally flattened exoskeleton suggests a benthic or nektobenthic mode of life for *L. deletres*, as for other trilobitomorphs, and it likely used its well-developed anteriorly positioned eyes for searching out food, either to scavenge or to find prey.

Keywords: Cambrian, Chengjiang biota, arthropod phylogeny, trilobitomorph, Xandarellida

1. Introduction

Some 250 species have been recorded from the Chengjiang biota, Cambrian Series 2, Stage 3 of Yunnan Province, South China, with arthropods being the most abundant and species-diverse group (Hou *et al.* 2017). These include some 18 arthropodan euarthropod species (*sensu* Ortega-Hernández *et al.* 2013), with representatives of the trilobitomorph groups Xandarellida, Trilobita, Nektaspida and Conciliterga. Here we describe a new xandarellid species from Chengjiang, *Luohuilinella deletres* sp. nov., preserved with dorsal exoskeleton and soft-part anatomy.

Four xandarellid species have previously been described, three from the Chengjiang biota and one from the middle Cambrian (Stage 5) of Morocco. They are assigned to three genera, *Cindarella* Chen, Ramsköld, Edgecombe & Zhou *in* Chen *et al.* (1996), *Xandarella* Hou *et al.* (1991), and *Luohuilinella* Zhang *et al.* (2012). The Moroccan *Xandarella mauretana* Ortega-Hernández *et al.* (2017) is known only from its soft-part anatomy; the type species *Luohuilinella rarus* from its dorsal exoskeleton; and the type species *Cindarella eucalla* and *Xandarella spectaculum* from their dorsal exoskeleton and soft-part anatomy.

The new species of *Luohuilinella* described here further elucidates the morphology of the eyes, gut and appendages of xandarellids.

2. Methods and material

The material of *L. deletres* is from Ercaicun, near Haikou town, Yunnan Province (Hou *et al.* 2017, fig. 4.3). It comprises three dorsoventrally flattened specimens and a single laterally flattened specimen (Figs 2-6). Type and figured specimens are housed in the collections of the Yunnan Key Laboratory for Palaeobiology, Yunnan University (numbers YKLP 11120a,b, 11121a,b, 11122a,b, and YKLP 11123a,b).

The anatomy of the new species was recorded using a camera lucida attached to a Wild Heerbrug M10 microscope. Macrophotography of the fossil material was undertaken using a Nikon D3X camera with a Af-S VR105 macro lens. The material was also imaged using a Hitachi S-3600N Scanning Electron Microscope at the School of Geography, Geology and the Environment, University of Leicester. Chemical analysis was undertaken using an Oxford INCA 350 EDX system, providing elemental mapping and point-and-ID spectrum. The system operated with a standard voltage of 15 kV; carbon was mapped using 5 kV.

Details of our phylogenetic analysis are presented in section 5.

3. Preservation

The appendages, eye and dorsal exoskeleton of *L. deletres* have been analysed for their mineralogy and chemical composition. The appendages are preserved as a coating of iron oxides after pyrite (see Gabbott *et al.* 2004, Zhu *et al.* 2005), comprised of a thin veneer of anhedral to subhedral microcrystals (usually 1.2 μm or less in diameter), and infrequent clusters of microcrystals and/or poorly-ordered framboids (Fig. 1a, b). At the distal tip of each lamella the iron oxides are distinctly larger than those in the proximal part of the appendage (the largest evident being 8.5 μm). Typically, a dark margin appears immediately beyond the appendage outline, which has the same chemical composition as the host matrix. Adjacent to this is a light grey region of mineralization, which is composed of Si, Al and K and minor amounts of Mg, and is likely to be the clay mineral illite, possibly of secondary origin.

The exoskeleton is markedly red against the yellow-coloured sediment. SEM analyses confirm that the red material is iron oxide, which densely coats the fossil. The iron oxides comprise mainly microcrystals and poorly ordered framboids. Some extremely small (less than a millimetre) patches of carbon can be resolved under high magnification scanning electron microscopy, although most carbon has oxidized, perhaps when the iron pyrites oxidized to iron oxides releasing H_2S . Some fine, exsagittally directed cracks occur on some of the pleurae (Fig. 1d).

The eye has some iron oxides in the form of microcrystals and poorly ordered framboids. However, these are few and scattered, unlike on the dorsal exoskeleton and appendages where they are very dense, and dense, respectively. Small carbon patches occur, but these are found beyond the fossil margin and are not exclusive to the eye.

Elemental mapping of the anatomy failed to discriminate any calcium, the absence of which is typical of the mode of preservation of Chengjiang fossils (Gabbott *et al.* 2004).

4. Systematic palaeontology

Phylum Euarthropoda Lankester, 1904
 Class? Artiopoda Hou & Bergström, 1997
 Order? Xandarellida Chen *et al.*, 1996
 Genus *Luohuilinella* Zhang, Fu & Dai, 2012

Diagnosis. Head shield one-third to one-fifth of total body length, with paired anterolateral eye notches. Trunk with between 27 to 30 tergites. Posterior of the antennae there are at least 11 pairs of biramous appendages, including three pairs in the head: exopods are slightly shorter than the endopods (Modified from Zhang *et al.* 2012).

Remarks. In their assessment of Xandarellida, Ortega-Hernández *et al.* (2017) noted that each tergite in the anterior half of the trunk covers a single pair of biramous appendages, whereas each succeeding tergite in the posterior half of the trunk covers an increasing number of appendage pairs. In *Luohuilinella* the posterior-most appendages are mostly not preserved.

Other xandarellids exhibit contrasting eye positions to that of *Luohuilinella*. In *Cindarella* the eyes protrude on slender stalks from beneath a head shield that lacks notches, whereas in *Xandarella* the eyes are set within dorsal slits in the head shield, well behind the anterior margin, while still being attached to the ventral body by stalks (Strausfeld *et al.* 2016, fig. 10).

In *Cindarella* the anterior trunk tergites are associated with a single pair of biramous appendages, but this pattern is decoupled beyond trunk tergite seven, where more than one somite is associated with each tergite. In *Luohuilinella* the first eight tergites are associated with a single trunk appendages, though with the exception of one exopod protruding beyond the terminal trunk tergite in YKLP 11123a,b (Fig. 5h), most of the more posterior appendages are not preserved. *Luohuilinella* differs from *Cindarella* by possessing anterolateral eye notches in the head shield, by its greater number of trunk tergites (27-30, versus 21-23), and by possessing three (as opposed to

four) pairs of biramous appendages in the head. *Luohuilinella* differs from *Xandarella* most notably in the position of its eyes (see above). In the type species *Xandarella spectaculum* there are six pairs of biramous appendages in the head behind the multi-segmented antennae, and the trunk has 12 tergites, the terminal one with a spine. The small (21 mm long including antennae) *X. mauretana* Ortega-Hernández *et al.* 2017 from Morocco, is known only from one specimen that lacks its dorsal exoskeleton. It has at least 22 pairs of post-antennal appendages, the first being about half the size of succeeding ones.

Luohuilinella deletres sp. nov.
(Figs 2-7)

Etymology. Greek, *deletron*, a lantern and *-es*, pertaining to; alluding to the stalked eyes.

Diagnosis. *Luohuilinella* with semi-elliptical head shield that is about one-fifth of the total body length, and with small eye notches relative to the size of the head shield. Trunk tergites are not separated by gaps abaxial to the narrow axial region and lack extended pleural spines. Axial region of trunk narrow and gradually tapering posteriorly of the fifth trunk tergite.

Holotype. A dorsoventrally preserved specimen, part and counterpart, YKLP 11120a,b. from Ercaicun, Haikou, Kunming; Yu'an Shan Member, Chiungchussu Formation, *Eoredlichia-Wutingaspis* trilobite biozone of eastern Yunnan, Nangaoan Stage of local usage, Cambrian Series 2, Stage 3.

Material. The holotype (Figs 2a, 5a-c,i), YKLP 11120a, b, and two other dorsoventrally preserved specimens (part and counterpart), YKLP 11121a,b and 11122a,b. A laterally preserved specimen, part and counterpart, YKLP 11123a,b.

Measurements. The exoskeleton of YKLP 11120a,b is 8.45 cm long excluding antennae, its head shield is 1.45 cm long, and its maximum width (at the fifth tergite) is 5.45 cm. The largest specimen, YKLP 11121a,b (Fig. 2b), is missing the posterior-most seven trunk tergites of the exoskeleton; it is 10 cm long as preserved, and 7 cm at

its maximum width (at the fifth tergite). The dorsal exoskeleton of this specimen likely approached 12 cm long.

Description. The dorsal exoskeleton possesses a semi-elliptical head shield that is about one-fifth of the total body length and has a rounded anterior margin, with the exception of two anterolateral notches that accommodate the eyes (Fig. 2a,b). The head shield lacks genal prolongations, sutures and surface sculpture. The hypostome is natant, with an elongate sub-oval outline (Fig. 2b). A moderately wide doublure is indicated inside the posterior, lateral and anterior margins of the head shield (Fig. 6b). The true inner margin of the doublure, and thus true width of the doublure, appears to be present near the posterior and one of the lateral margins of the head shield; near the other lateral margin and anteriorly between the eye notches, the inner margin of the doublure is much more irregular, indicating decay in these areas, resulting here in a narrower doublure. A pair of laterally placed stalked eyes project just in front of the anterior margin of the head shield, anterior of which and extending well beyond the edge is a pair of slender uniramous antennae, each with at least 26 podomeres (Fig. 2a). Posterior to the antennae there are at least 11 pairs of biramous appendages preserved, including three pairs in the head (Fig. 3a). The first two post-antennal appendages appear to be shorter than succeeding appendages (Fig. 3a). Each of the appendages comprises a slender endopod that may bear ten podomeres (Figs 3d,d1, 4a,b), lacking endites. The exopods are paddle shaped distally, slightly shorter than the endopods, and have flat lamellae (Fig. 5e,f). Paired tubular diverticula are present along the mid-gut, being transversely wider beneath the head shield and gradually narrowing posteriorly (Fig. 3e).

The trunk has a distinctly convex axial region, demarcated from the pleural regions by a weak axial furrow (Figs 2a,b, 5c,i, 6a). It is composed of 30 tergites, the first small and axial, and partly overlapped by the posterior margin of the head shield. The trunk tergites are well defined; abaxially they are progressively more reflexed backwards posteriorly, so that the terminal five tergites with pleural elongations (tergites 23-27) curve and project directly backwards (Fig. 2a). Tergites 2-27 terminate abaxially in a pleural spine, these are short anteriorly in the trunk, becoming progressively longer posteriorly, and the abaxial, gently convex edge of each tergite bears 15 tiny serrations (Fig. 6a). The trunk is weakly abaxially convex in outline and

tapers gradually posteriorly of tergite five. The terminal three tergites are axial, each without a pleural extension, and there is a stout terminal spine.

Remarks. The type species of *Luohuilinella*, *L. rarus*, possesses paired anterior notches in its head shield and, despite the absence of soft-part anatomy, Zhang *et al.* (2012) correctly interpreted these features as ‘accommodating ventral eyes’. The only specimen of *L. rarus*, which is also from the Chengjiang biota, is 16.8 mm long and 8.8 mm wide. The head shield is elongate sub-elliptical with acute genal angles and is approximately one-third of the total length of the exoskeleton. It has a glabella that terminates well behind the eye notches, and a posteriorly narrowing trunk with well-defined axial and pleural regions, which Zhang *et al.* (2012) recorded as having 27 tergites and a terminal piece. *L. deletres* is distinguished from *L. rarus* by the markedly different shape of its head shield, which is semi-elliptical and about one-fifth of the length of the exoskeleton; its trunk tergites, which are not separated by gaps abaxial to the axial region; the shape of the axis, which is narrower and less tapering posteriorly; the smaller size of its eye notches relative to the size of the head shield; and by possessing 30 tergites (comprising an anterior-most (first) axial tergite, 26 tergites with pleural elongations, and 3 terminal tergites without these elongations).

There is a patchy darker region (Fig. 6b,f) surrounding the elongate-oval, natant hypostome of *L. deletres* (Fig. 2b), but nothing that we could confidently identify as a specific structure.

The three terminal tergites that lack pleural extensions in *L. deletres* resemble a pygidium (Figs 2a, 3a, 5b), though we cannot determine if the segments are fused or articulated. In its small size this structure resembles the micropygous pygidium of redlichiid trilobites and its segments are markedly different from those of trunk segments 2-27 in lacking a pleural component. The terminal three tergites and terminal piece of *L. rarus* also lack pleural extensions and may represent a homologous structure.

The full morphology of the exopod of *L. deletres* is unclear. In YKLP 11123a,b the distal end is paddle-shaped (Figs 1a, 5e,f), and bears closely spaced flat lamellae. We cannot discern whether these lamellae are morphologically uniform along the length of the exopod. In the single biramous appendage visible in the head of YKLP11121a,b, the distal lamellae of the exopod are narrow and short (Figs 2b, 6a,b,d, f). More proximally on this exopod there appear to be longer structures that

resemble spines (Figs 2b, 6b,f), but we cannot be certain whether these are derived from the exopod, or from another, associated structure.

5. Phylogenetic affinity

To evaluate the evolutionary significance of the new anatomical data yielded by *L. deletres*, the new species was added to the phylogenetic study of Siveter *et al.* (2017). This dataset has extensive taxonomic coverage of arthropods including artiopodans. *L. deletres* has been coded for the subset of characters found to be informative for trilobitiform and vicissicaudate taxa as defined by Siveter *et al.* (2014; see Supplementary Information) using the character list taken from an earlier version of this dataset (Siveter *et al.* 2014). Coding for *Acanthomeridion* was also updated, to reflect data from Hou *et al.* (2016). The new dataset (Supplementary Information) was analysed using Bayesian analysis in MrBayes (standard morphological data, with variable coding, gamma rates, 4 chains, 16 million generations, see Supplementary Information for details; Ronquist *et al.* 2011).

Tree searches using Bayesian analysis resolved a xandarellid affinity for *L. deletres* and *L. rarus* as they are placed in a clade with *Cindarella* and *Xandarella* (Fig. 8). This placement is supported by the presence of head shield articulation with a reduced trunk tergite (character 44), strongly curved posterior tergites (character 108), and the presence of eye slits (character 363) (the latter being homoplastic). The relationships within Artiopoda largely mirror those recovered in the analyses of Lerosey-Aubril *et al.* (2017) in that Xandarellida is in a clade with Trilobita and Nektaspidida, but the new result is equivocal with respect to the monophyly of ‘Petalopleura’ and the placement of *Sinoburius*. The relationships in other parts of the consensus tree are less resolved; the major arthropod clades form a polytomy that includes a wide range of Cambrian taxa, including *Acanthomeridion*. Alternative searches using parsimony in TNT (Goloboff *et al.* 2008a,b) find poor resolution among artiopodan taxa both with and without the application of implied weighting, or the inclusion or exclusion of *Habelia* (not figured).

Recent simulation studies have suggested that Bayesian analyses are more accurate than parsimony analyses, and that the latter provide false precision (especially with implied weighting) (Wright & Hillis 2014; O’Reilly *et al.* 2016; although see Goloboff *et al.* 2017). Our analyses of new and updated empirical data for arthropods indicate that the results from Bayesian searches provide resolution for

the parts of the tree in question here, but yield unconventional results in other parts of the tree (i.e. monophyletic Atelocerata, paraphyletic Chelicerata and monophyly of clades previously interpreted as successive stem-arthropod plesia, Supplementary Information). Similar results were obtained in the Bayesian analysis of Wolfe (2017). Maximum parsimony searches, however, yielded even less resolved consensus trees (including failing to recover monophyletic Artiopoda). Parsimony searches were very sensitive to taxon inclusion and character weighting. Furthermore, taxon inclusion and character weighting interact in searches with implied weighting in that the relationships and resolution in one part of the tree are affected by taxon exclusion in distant parts of the tree. Future studies would benefit from total evidence analysis (simultaneous analysis of morphological and molecular data) and from focus on character coding of trilobitomorpha taxa, some of which may be acting as ‘wildcard’ taxa.

6. Palaeoecology

Luohuilinella deletres is a rare component of the Chengjiang biota and is only recorded from rapidly deposited so-called ‘Event Beds’ (for which see Hou *et al.* 2017) at a single locality, Ercaicun. Other xandarellids in the Chengjiang biota are also rare. *Luohuilinella rarus* is known only from one specimen, at Mafang (Zhang *et al.* 2012). *Cindarella eucalla* and *Xandarella spectaculum* are known from a few tens of specimens, but are always rare components of fossil assemblages (Hou *et al.* 2017). Until recently xandarellids were known exclusively from the Chengjiang biota. The discovery of a xandarellid in the middle Cambrian (Stage 5) of Morocco suggests a much wider biogeographical reach from the early Palaeozoic continents of South China to Gondwana (Ortega-Hernández *et al.* 2017). It is unclear whether xandarellids were rare components of arthropod assemblages more generally, or whether they are under-represented in these Lagerstätten because of taphonomic/palaeoenvironmental biases.

As in other trilobitomorpha the dorsoventrally flattened exoskeleton suggests a benthic or nektobenthic mode of life for *L. deletres* (see Hou *et al.* 2017, fig. 6.2). If it lived at or near the seabed, it likely used its well-developed anteriorly positioned stalked eyes for searching out food, either to scavenge or to find prey. The eyes may have had sophisticated capabilities. Those of the closely related *Cindarella* are

reconstructed as having more than 2,000 ommatidia, a differentiated bright zone, and a near-spherical visual field (Zhao *et al.* 2013). However, the consistent and close association of the eyes with the marginal notches of the head shield in *L. deletres* suggests a more limited range of eye movement than in *Cindarella*, potentially reducing the ability to stabilise the visual field during rapid movement (cf. Schoenemann 2006). Even so, the eyes of *L. deletres* are likely to have had a greater range of movement than those of *Xandarella*, which appear to have been tightly integrated into the dorsal head shield during life (see Strausfeld *et al.* 2016, fig. 10). As a group, therefore, xandarellids exhibit a variety of eye positions that are likely to represent trade-offs between visual-range, stability of the visual field, and degree of protection from predation or other physical damage to the eyes. A full account of the evolution of eye position among trilobitomorpha requires a better-resolved phylogeny. However, given that stalked eyes are likely to be plesiomorphic for euarthropods (Strausfeld *et al.* 2016), the marginal, socketed eye positions of *L. deletres* may record an intermediate condition in a trend towards progressive integration of the eyes into the head shield of trilobitomorpha, which is more fully expressed in *Xandarella* and (presumably by convergence) in trilobites.

The extensively preserved digestive system of *L. deletres* potentially offers additional insights into diet and palaeoecology. The overall architecture, with a midline gut producing lateral, unbranched diverticula that are transversely wider towards the front of the body, recalls that of various trilobites (e.g., Chatterton *et al.* 1994; Lerosey-Aubril *et al.* 2012, 2017; Gutiérrez-Marco *et al.* 2017). Many extant arthropods with extensive diverticula are fluid feeders (i.e., predators with rich but intermittent intake of food or fluidised food), and the evolution of complex digestive systems has more generally been linked to the rise of predatory and scavenging behaviour (e.g., Vannier *et al.* 2014). It is notable that the tubular gut diverticula of *Luohuilinella* are distinctly different from the reniform diverticula of *Cindarella*, perhaps indicating distinctive feeding habits in different xandarellid taxa.

7. Conclusions

Luohuilinella deletres is the fourth xandarellid species to be described from the Chengjiang biota of South China. It provides additional anatomical evidence of the exoskeletal, eye, appendage, and gut morphology for *Luohuilinella*, and confirms that the anteriorly situated notches in the head shield are associated with the eyes,

potentially informing on evolutionary trends in eye position. In having lateral, unbranched diverticula that are wider towards the front of the body, the midline gut of *L. deletres* is like that of various trilobites.

Acknowledgements

We acknowledge funding for this research from the National Natural Science Foundation of China (Grant numbers U1302232, 41372031, and 41528202), the Royal Society (Grant number IE131457), and the Leverhulme Trust (Grant number EM-2014-068). We thank Dayou Zhai (of YKLP) for measuring the fossils, and Javier Ortega-Hernández and an anonymous reviewer for their detailed comments on the manuscript. This publication is undertaken under the auspices of the MEC International Joint Laboratory for Palaeobiology and Palaeoenvironment, Yunnan University, China.

Supplemental data

Supplemental data (document 1 – tnt formatic matrix, and 2, nexus file, with majority rules consensus tree from Bayesian Analysis and Mr Bayes) to support the phylogenetic analyses (see Figure 8) and can be accessed at the online version of this manuscript and at Dryad (data can only be uploaded following acceptance).

References

- BRIGGS, D.E.G., SIVETER, DEREK J., SIVETER, DAVID J., SUTTON, MARK D. & LEGG, D. 2016. Tiny individuals attached to a new Silurian arthropod suggest a unique mode of brood care. *PNAS*, **113**, 4410-4415.
- CHATTERTON, B.D.E., JOHANSON, Z. & SUTHERLAND, G. 1994. Form of the trilobite digestive system: alimentary structures in *Pterocephalia*. *Journal of Paleontology*, **68**, 294–305.
- CHEN, J.-Y., ZHOU, G.-Q., ZHU, M.-Y. & YEH, K.-Y. 1996. *The Chengjiang biota. A unique window of the Cambrian explosion*. 222 pp. National Museum of Natural Science, Taichung, Taiwan. [In Chinese].
- GABBOTT, S.E., HOU, X.-G., NORRY, M.J. & SIVETER, D.J. 2004. Preservation of Early Cambrian animals of the Chengjiang biota: *Geology*, **32**, 901–904.

- GOLOBOFF, P.A., FARRIS, J.S. & NIXON, K.C. 2008a. TNT, a free program for phylogenetic analysis. *Cladistics*, **24**, 774–786.
- GOLOBOFF, P.A., CARPENTER, J.M., ARIAS, J.S. & MIRANDA ESQUIVEL, D.R. 2008b. Weighting against homoplasy improves phylogenetic analysis of morphological data sets. *Cladistics*, **24**, 1–16.
- GOLOBOFF, P. A., TORRES, A. & ARIA, J. S. 2017. Weighted parsimony outperforms other methods of phylogenetic inference under models appropriate for morphology. *Cladistics*, doi:10.1111/cla.12205.
- GUTIÉRREZ-MARCO, J.C., GARCÍA-BELLIDO, D.C., RÁBANO, I. & SÁ, A.A. 2017. Digestive and appendicular soft-parts, with behavioural implications, in a large Ordovician trilobite from the Fezouata Lagerstätte, Morocco. *Scientific Reports*, **7**, 39728.
- HOU, X.-G. & BERGSTROM, J. 1997. Arthropods of the Lower Cambrian Chengjiang fauna, southwest China. *Fossils and Strata*, **45**, 1-116.
- HOU X.-G., RAMSKÖLD, L. & BERGSTRÖM, J. 1991. Composition and preservation of the Chengjiang fauna - a Lower Cambrian soft-bodied biota. *Zoologica Scripta*, **20**, 395-411.
- HOU, X.-G., WILLIAMS, M., GABBOTT, S., SIVETER, DAVID J., SIVETER, DEREK J., CONG, P.-Y., MA, X.-Y. & SANSOM, R. A new species of the artiopodan arthropod *Acanthomeridion* from the lower Cambrian Chengjiang Lagerstätte, China, and the phylogenetic significance of the genus. *Journal of Systematic Palaeontology*, **15**, 733-740.
- HOU, X.-G., SIVETER, DAVID J., SIVETER, DEREK J., ALDRIDGE, R.J., CONG, P.-Y., GABBOTT, S.E., MA, X.-Y., PURNELL, M. & WILLIAMS, M. 2017. The Cambrian fossils of Chengjiang, China: the flowering of early animal life. Wiley-Blackwell, Oxford, 328 pp.
- LANKESTER, E.R. 1904. The structure and classification of Arthropoda. *Quarterly Journal of Microscopical Science*, **47**, 523–582.
- LEGG, D.A., SUTTON, M.D. & EDGECOMBE, G.D. 2013. Arthropod fossil data increase congruence of morphological and molecular phylogenies. *Nature Communications*, doi 10.1038/ncomms3485.
- LEGG, D.A., SUTTON, M.D., EDGECOMBE, G.D. & CARON, J.-B. 2012. Cambrian bivalved arthropod reveals origin of arthropodization. *Proceedings of the Royal Society*, **B279**, 4699-4704.

- LEROSEY-AUBRIL, R., HEGNA, T.A., KIER, C., BONINO, E., HABERSETZER, J. & CARRÉ, M. 2012. Controls on gut phosphatisation: the trilobites from the Weeks Formation Lagerstätte (Cambrian; Utah). *PLoS ONE* **7**, e32934.
- LEROSEY-AUBRIL, R., PATERSON, J.R., GIBB, S. & CHATTERTON, B.D.E. 2017. Exceptionally-preserved late Cambrian fossils from the McKay Group (British Columbia, Canada) and the evolution of tagmosis in aglaspidid arthropods. *Gondwana Research*, **42**, 264–279.
- O'REILLY, J., PUTTICK, M. N., PARRY, L. A., TANNER, A., TARVER, J. E., FLEMING, J., PISANI, D. & DONOGHUE, P. C. J. 2016. Bayesian methods outperform parsimony methods but at the expense of precision in the estimation of phylogeny from discrete morphological data. *Biology Letters*, **12**, 20160081.
- ORTEGA-HERNÁNDEZ, J., LEGG, D.A. & BRADY, S.J. 2013. The phylogeny of aglaspidid arthropods and the internal relationships within Artiopoda. *Cladistics*, **29**, 15-45.
- ORTEGA-HERNÁNDEZ, J., AZIZI, A., HEARING, T. W., HARVEY, T. H. P., EDGECOMBE, G. D., HAFID, A. & EL HARIRI, K. 2017. A xandarellid artiopodan from Morocco – a middle Cambrian link between soft-bodied euarthropod communities in North Africa and South China. *Scientific Reports*, **7**, 42616.
<http://doi.org/10.1038/srep42616>
- RAMSKÖLD, L., CHEN, J.-Y., EDGECOMBE, G.D. & ZHOU, G.-Q. 1997. *Cindarella* and the arachnate clade Xandarellida (Arthropoda, Early Cambrian) from China. *Transactions of the Royal Society of Edinburgh: Earth Sciences*, **88**, 19-38.
- RONQUIST, F., TESLENKO, M., VAN DER MARK, P., AYRES, D. L., DARLING, A., HÖHNA, S., LARGET, B., LIU, L., SUCHARD, M. A. & HUELSENBECK, J. P. 2011. MrBayes 3.2: Efficient Bayesian phylogenetic inference and model choice across a large model space. *Systematic Biology*, **61**, 539-542.
- SCHOENEMANN, B. 2006. Cambrian view. *Palaeoworld* **15**(3), 307–314.
- SIVETER, DEREK J., BRIGGS, D.E.G., SIVETER, DAVID J., SUTTON, M.D., LEGG, D. & JOOMUN, S.C. 2014. A Silurian short-great-appendage arthropod. *Proceedings of the Royal Society London*, **B281**, 20132986.
- SIVETER, DAVID J., BRIGGS, D.E.G., SIVETER, DEREK J., SUTTON, M.D. & LEGG, D. 2017. A new crustacean from the Herefordshire (Silurian) Lagerstätte, UK, and its significance in malacostracan evolution. *Proceedings of the Royal Society London*, **B284**, 2017029.

- STRAUSFELD, N.J., MA, X.-Y., EDGECOMBE, G.D., FORTEY, R.A., LAND, M.F., LIU, Y., CONG, P.-Y. & HOU, X.-G. 2016. Arthropod eyes: the early Cambrian fossil record and divergent evolution of visual systems. *Arthropod Structure & Development* **45**, 152–172.
- VANNIER, J., LIU, J., LEROSEY-AUBRIL, R., VINTHER, J. & DALEY, A. 2014. Sophisticated digestive systems in early arthropods. *Nature Communications*, **5**, 3641 doi: 10.1038/ncomms4641
- WOLFE, J. M. 2017. Metamorphosis is ancestral for crown euarthropods, and evolved in the Cambrian of earlier. *Intergrative and Comparative Biology*, doi: 10.1093/icb/icx039.
- WRIGHT, A. M. & HILLIS, D. M. 2014. Bayesian analysis using a simple likelihood model outperforms parsimony for estimation of phylogeny from discrete morphological data. *PLoS ONE*, **9**, e109210.
- ZHANG, X.-L., FU, D.-L. & DAI, T. 2012. A new xandarellid arthropod from the Chengjiang Lagerstätte, Lower Cambrian of southwest China. *Geobios*, **45**, 335–338.
- ZHAO, F.-C., BOTTJER, D.J., HU, S.-X., YIN, Z.-J. & ZHU, M.-Y. 2013. Complexity and diversity of eyes in Early Cambrian ecosystems. *Scientific Reports* **3**, 2751, doi: 10.1038/srep02751.
- ZHU, M.-Y., BABCOCK, L.E. & STEINER, M. 2005. Fossilization modes in the Chengjiang Lagerstätte (Cambrian of China); testing the roles of organic preservation and diagenetic alteration in exceptional preservation. *Palaeogeography, Palaeoclimatology, Palaeoecology*, **220**, 31–46.

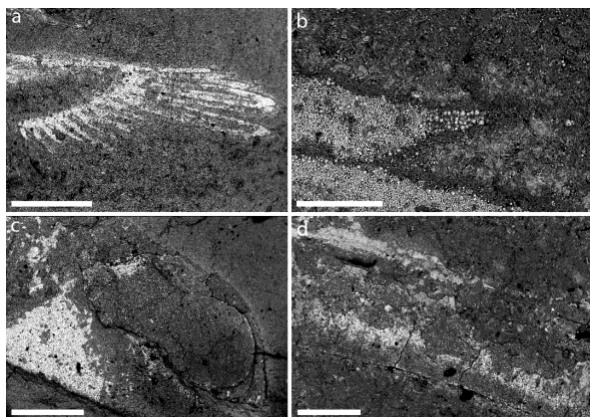
Figures

Figure 1. Taphonomy of *Luohuilinella deletres*. a-d, back-scattered electron images of specimen 11123a,b. a, appendage showing iron oxide (after pyrite) as bright minerals coating anatomy including lamellae. Scale bar is 1mm. b, lamellae showing that iron oxides in the distal tip are frequently larger than those in the proximal part of the appendage. The dark margin seen around the lamellae is typical. Scale bar is 100 microns. c, Kidney-shaped eye showing preservation in relief, rather than as a coating of iron oxides. Scale bar: 1 mm. d, fine, exsagittally directed cracks on pleura. Scale bar is 500 microns.

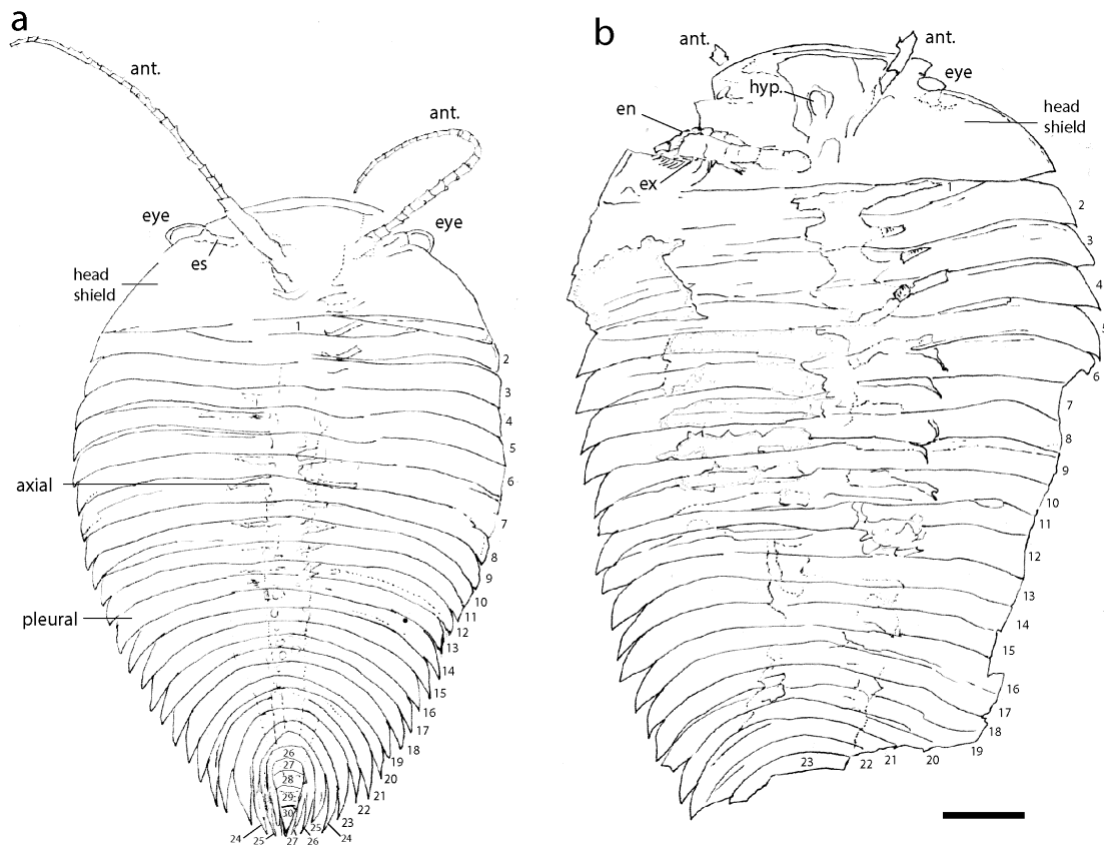


Figure 2. Camera lucida interpretation of two dorsoventrally preserved specimens of *Luohuilinella deletres*. a, holotype YKLP 11120a. b, posteriorly incomplete specimen YKLP11121a. Abbreviations: ant, antenna; hyp, hypostome; en, endopod; ex, exopod. Scale bar (bottom right): 1 cm for both specimens. Numbers refer to trunk tergites.

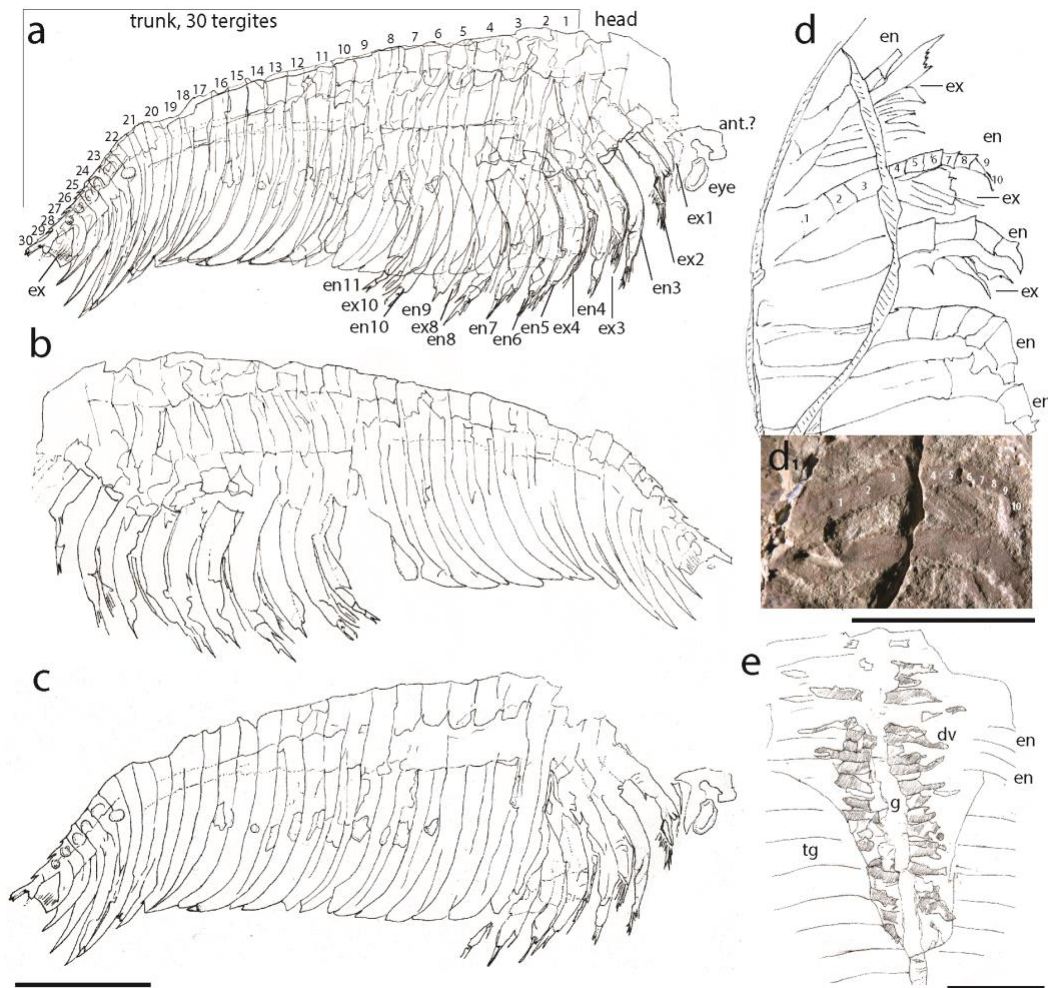


Figure 3. Camera lucida and photographic interpretation of two specimens of *Luohuilinella deletres*. a-c, laterally preserved specimen: a, composite of 11123a,b; b, YKLP 11123a; c, YKLP 11123b. d, d1, e, YKLP 11122a,b dorsoventrally preserved specimen with appendages (part), and gut (counterpart specimen) respectively. Abbreviations as for Fig. 2, plus: tg, tergite; dv, gut diverticula; numbers 1-10 in 'd' and 'd1' are interpreted as podomeres (see also Fig. 4). In Figure 3a the position of the head-thorax boundary is based on there being 30 trunk-tergites posterior of this (numbered). All scale bars are 1 cm. Bottom left scale bar applies to images a-c.

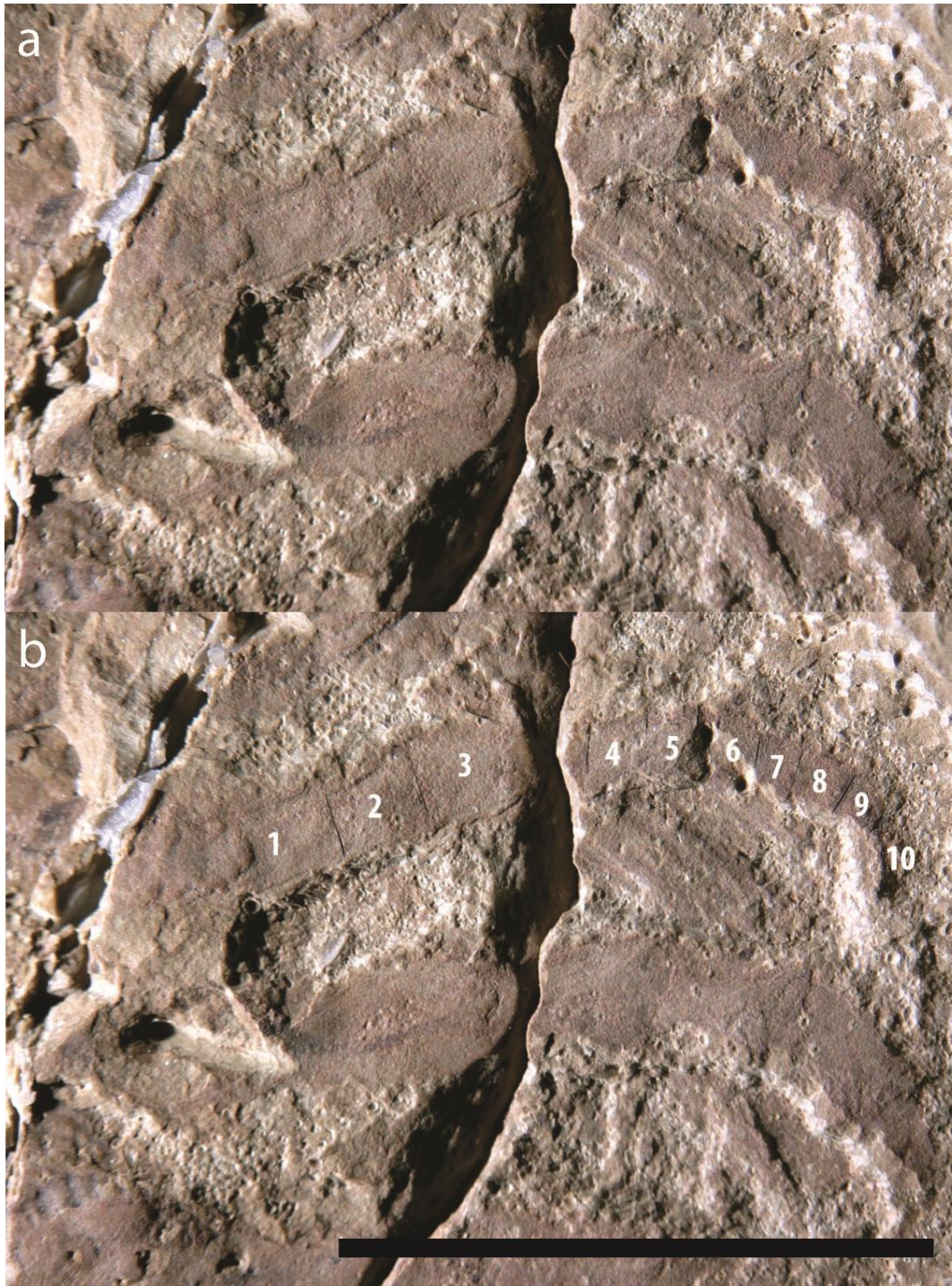


Figure 4. a, b, close-up of endopods in specimen YKLP 11122b, see also Figure 3d, d1. Numbers 1-10 are interpreted as podomeres, with the podomere boundaries emphasised in the lower panel b. We note that in adjacent endopods the boundaries of podomeres are indistinct. Scale bar is 1 cm.

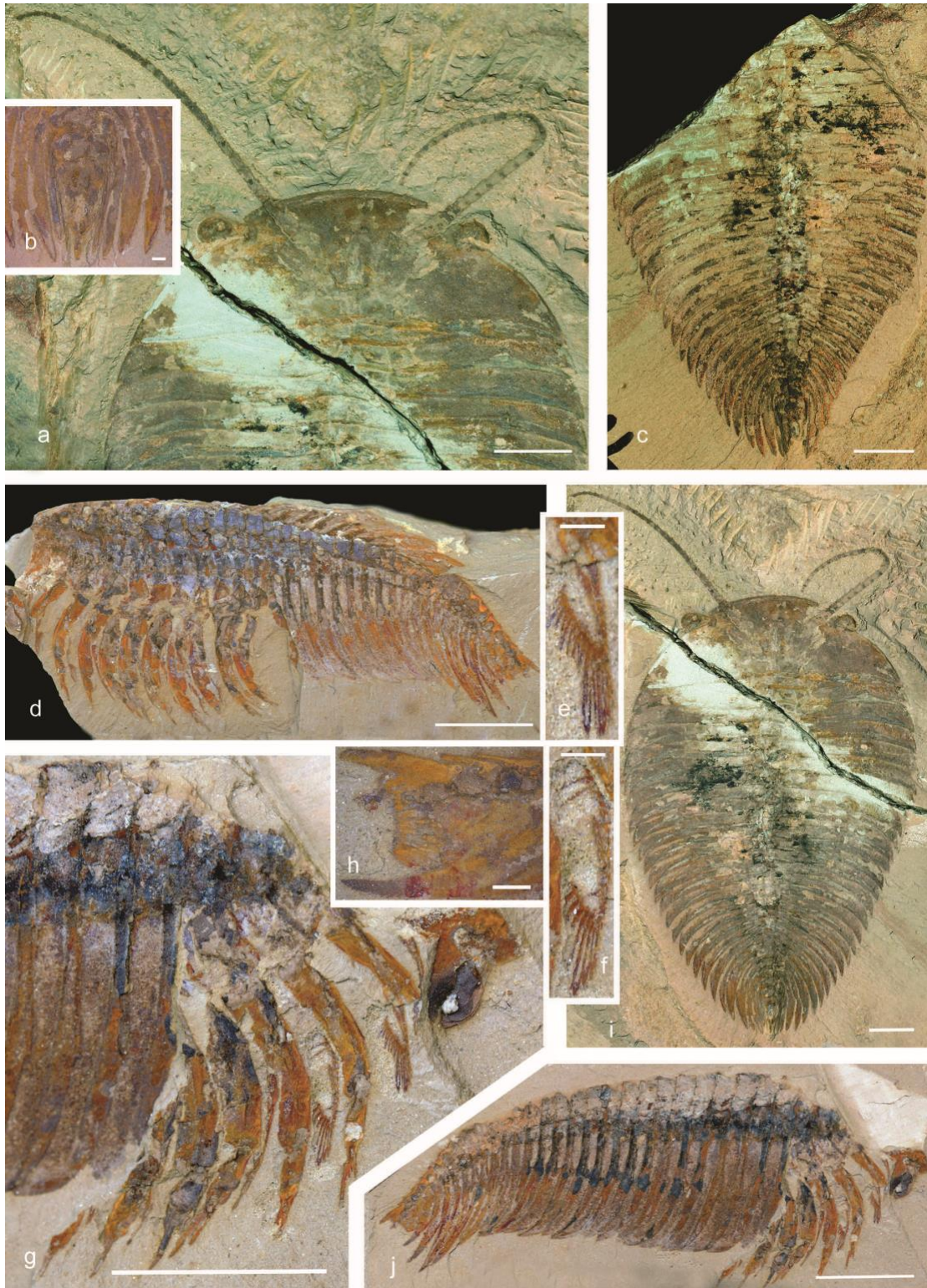


Figure 5. Photographic images of two specimens (parts and counterparts) of *Luohuilinella deletres*, preserved laterally (d-h, j), and dorsoventrally (a-c, f). a, b, i, close-ups of anterior and posterior, and view of whole specimen, YKLP 11120a. c, counterpart whole specimen YKLP 11120b. d, specimen YKLP 11123a. e, f, g, h, j,

close-up of two exopods (see g for their positions), anterior, posterior with displaced, exposed exopod, and whole specimen, YKLP 11123b. Scale bars for a, c, d, i, g, j: 1 cm; for b, e, f, h: 1mm. See Figs 2 and 3 for labelled features.

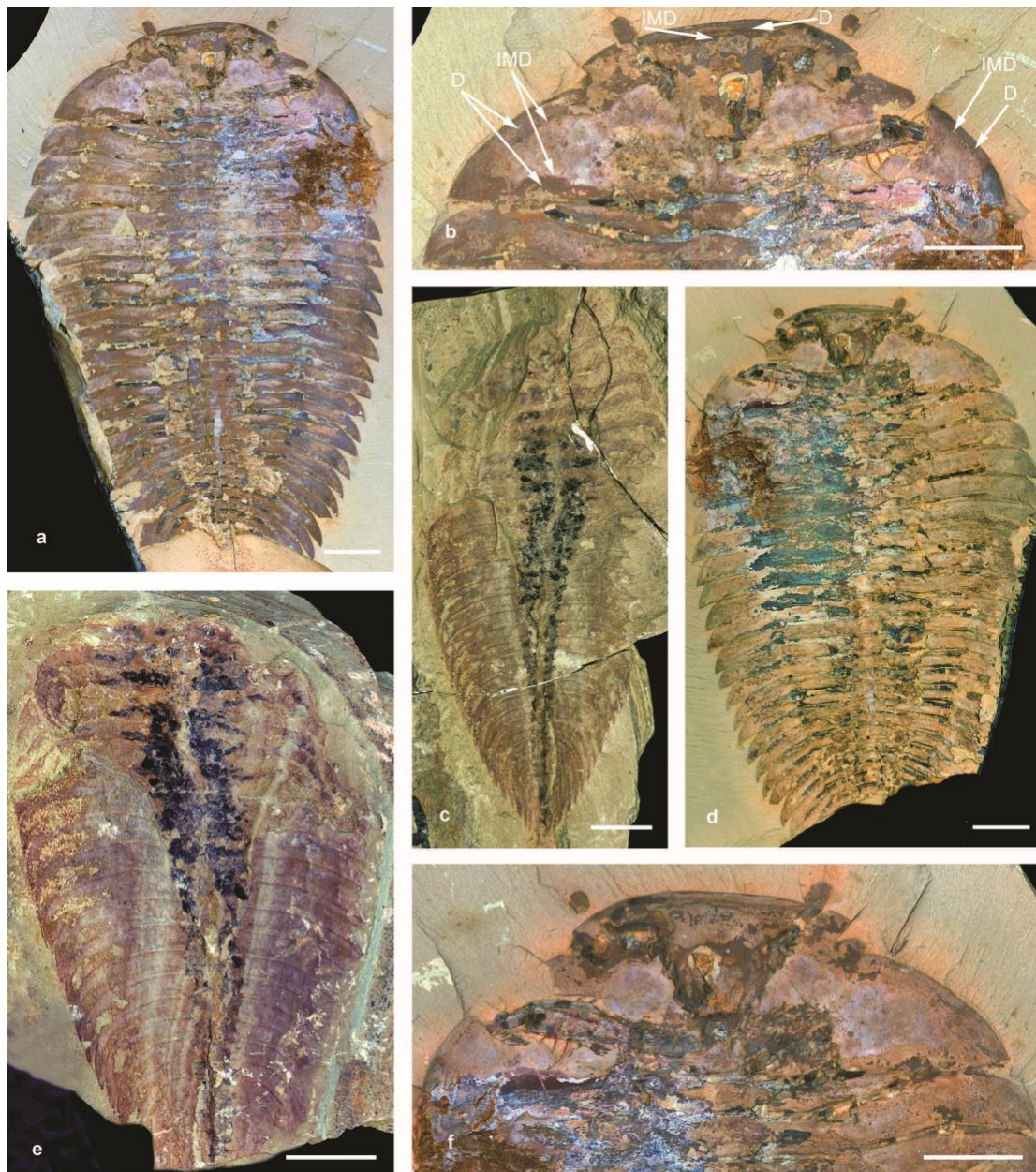


Figure 6. Photographic images of two specimens of *Luohuilinella deletres* (parts and counterparts) preserved dorsoventrally. a, b, counterpart, posteriorly incomplete specimen, whole view and close up of anterior, YKLP11121b: note this specimen and its counterpart (6d,f) shows the only well-preserved biramous limb in the head. d, f, whole specimen and anterior of part, YKLP11121a. c, e, part and counterpart, YKLP

11122a,b, showing trace of gut. All scale bars: 1 cm. Abbreviations: D, doublure; IMD, inner margin of doublure. See Figures 2 and 3 for other labelled features.

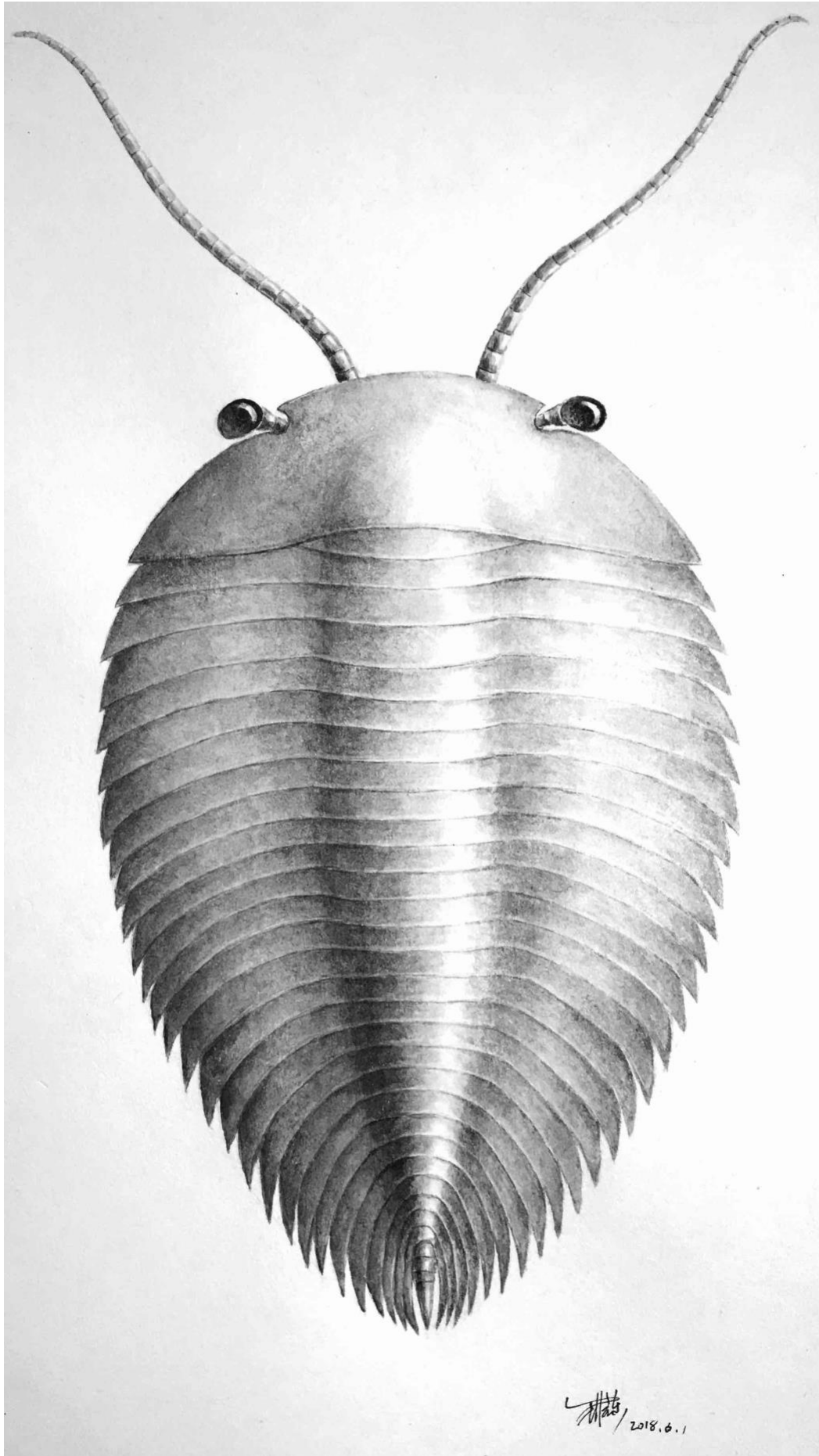


Figure 7. Reconstruction of *Luohuilinella deletres* (based largely on YKLP 11120a, for which see Figs 2a, 5a, i).

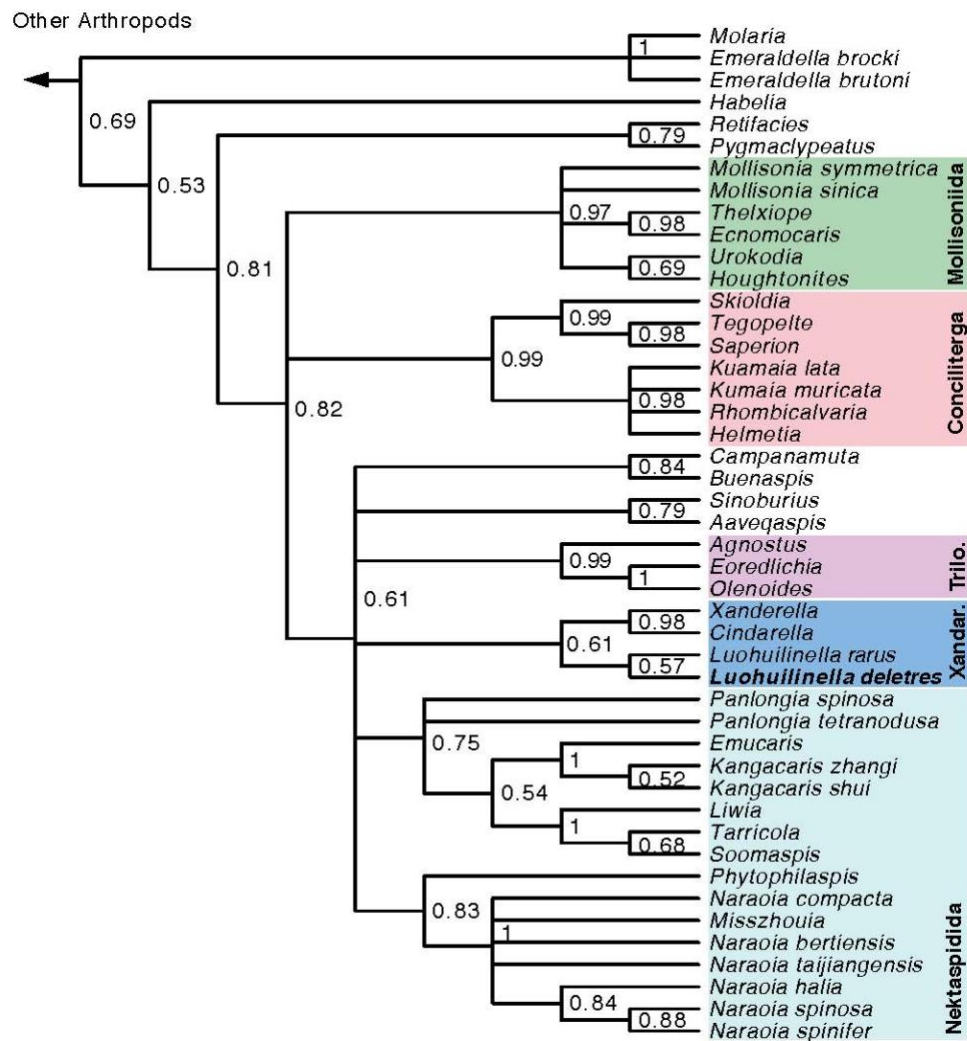


Figure 8. Phylogeny of Trilobitomorpha under Bayesian analysis (50% majority rule consensus tree). *Luohuilinella deletres* and *L. rarus* are recovered as xandarellids. The selection of taxa relevant to artiopodan relationships are shown, with the root and other arthropods condensed.